Indian Journal of Biochemistry & Biophysics
Vol. 62, February 2025, pp. 178-186
DOI: 10.56042/ijbb.v62i2.13314

Identification of novel compound against STAT3 mediated liver fibrosis: An MD simulation based study

Doli Saloi, Nerswn Basumatary, Trisha Sonowal & Jatin Sarmah*

Department of Biotechnology, Bodoland University, Deborgaon-783 370, Assam, India

Received 22 August 2024; *revised 09 September 2024*

Liver fibrosis, characterized by the pathological accumulation of extracellular matrix in response to chronic liver injury, represents a significant global health concern. Signal Transducer and Activator of Transcription 3 (STAT3) have been identified as a critical mediator in the fibrotic process, making it an attractive target for therapeutic intervention. This study aimed to computationally design a novel inhibitor against STAT3, utilizing bioactive compounds derived from *Ricinus communis*, a plant recognized for its hepatoprotective properties. 30 bioactive compounds from *Ricinus communis* were initially screened through molecular docking with STAT3, followed by further evaluation of the top 10 compounds using Swiss ADME for pharmacokinetic parameters and drug-like properties. Subsequently, (5beta)Pregnane-3,20beta-diol, 14alpha, 18alpha-[4-methyl-3-oxo-(1-oxa-4-azabutane-1,4-diyl)]-, diacetate was selected based on its robust binding affinity and favorable Swiss ADME profile, demonstrating potential stability in complex with STAT3 through molecular dynamics (MD) simulations. Analysis of MD simulation trajectories indicated stable interactions between STAT3 and (5beta)Pregnane-3,20beta-diol, 14alpha,18alpha-[4-methyl-3-oxo-(1-oxa-4-azabutane-1,4-diyl)]-, diacetate, as evidenced by RMSD, RMSF, Rg, SASA and binding free energy values. In conclusion, These findings position (5β)Pregnane-3,20β-diol, 14α.,18α.-[4-methyl-3-oxo-(1-oxa-4-azabutane-1,4-diyl)]-diacetate as a promising inhibitor of STAT3 from *Ricinus communis*, offering potential for therapeutic advancement in liver fibrosis treatment and drug development.

Keywords: ADME, MD simulations, Molecular docking, *Ricinus communis*

Chronic liver injury combined with an excessive build-up of extracellular matrix (ECM) proteins, such as collagen, results in liver fibrosis[1]. Severe liver fibrosis can lead to complications like cirrhosis and liver failure, which ultimately may be corrected by liver transplant. Chronic hepatitis C virus (HCV) infection, alcohol misuse, and nonalcoholic steatohepatitis (NASH) are the major causes of liver fibrosis, which constantly damages the hepatocytes. Liver fibrosis and cirrhosis are reversible wound-healing responses to chronic liver damage, forming regenerative nodules when hepatocytes are constantly injured. Liver fibrosis is primarily caused by activated hepatic stellate cells (HSCs), portal fibroblasts, and myofibroblasts originating from bone marrow. These cells secrete collagen[2]. Active HSCs develop a myofibroblast (α-SMA)--like phenotype, which proliferates, becomes fibrogenic, and produces a large amount of ECM proteins[3]. In a healthy liver, the portal fibroblasts provide structural functions such as stabilizing the hepatic ducts; nevertheless, in the event of an injury, they take part in fibrosis and wound healing[4]. Liver fibrosis in a mouse model can be decreased by inhibiting TGF-β1, a cytokine that promotes fibrogenesis[5]. This suggests that inhibiting TGFβ1 signal transduction could be a potential therapeutic target for liver fibrosis. Additionally, inhibiting STAT3, a target gene for liver fibrosis, could reduce anginogenesis and further fibrogenesis. Rapid activation of STAT3 has been observed in HSCs and fibroblasts compared to other hepatocytesTGF-B1, a STATE3 target gene, has been shown to activate STAT3 quickly in HSCs and to induce liver fibrosis by up regulating TGF-B1 expression in a mouse model of hepatic fibrosis. Thus, blocking STAT3 may be a therapeutic strategy for liver fibrosis as it may also lower anginogenesis and subsequent fibrogenesis[6]. N-acetylcysteine (NAC) has been identified as a potent inhibitor of hepatic stellate cell (HSC) activation, with significant implications for attenuating liver fibrosis in a carbon tetrachloride (CCl_4)-induced rat model of hepatic

*Correspondence:
Phone: 0091-97071-75220
E-mail: jatinsarmahindia@gmail.com

injury[7]. Galunisertib, a selective inhibitor of TGF-β receptor type I kinase, plays a critical role in modulating the fibrogenic pathway by attenuating TGF-β-mediated signaling[8].

Despite significant advances in the molecular mechanisms underlying liver fibrosis, effective therapeutic interventions remain limited. Thus, studies on several traditional remedies derived from plants are being conducted to assess their hepatoprotective properties against chemically induced liver injury in laboratory animals[9]. *Ricinus communis*, commonly known as the castor plant` has been extensively studied for its hepatoprotective properties[10]. Native to tropical Africa, it is found in countries like India, China, Brazil, and the Southern US. The ab-orgin populations like Kani of Tamil Nadu and the Chenchu and Yerukula of Andhra Pradesh utilize it for various liver ailments[11,12]. For many years, aborigines of Assam used aqueous extract of *Ricinus communis*, as a medicine for different liver disorders[13]. Leaf extract of the plant were found to be effective in protecting liver from damage induced by toxins such as carbon tetrachloride and d-galactosamine in mice[14]. Liver damage in mice closely resembles human chronic liver damage in their morphological and functional features[15]. *Ricinus communis* has potential therapeutic applications in treating hepatitis and liver fibrosis[11]. The plant's entire leaf extract, when diluted with various solvents, protects against liver necrosis and the fatty alterations brought on by CCL4[16]. The presence of strong antioxidants, *viz*. rutin, gentisic acid, quercetin, gallic acid, ellagic acid, and epicatechin, is thought to have hepatoprotective activity against liver fibrosis[17].

Molecular docking is a computational modeling technique that generates thousands of preferred binding poses between a ligand and a receptor molecule, forming a stable complex[18]. This study utilized molecular interaction studies and docking to identify potential molecules from *Ricinus communis* inhibiting the STAT3 protein, predicting their binding affinities using scoring functions.

This study focuses on identifying the potential drug candidate for the liver fibrosis using the bioactive compounds of the plant *Ricinus communis* using computational methods.

Materials and Methods

Compound retrieval

The bioactive compounds used in this study were carefully chosen by thoroughly reviewing significant research papers and databases. The plant *Ricinus communis*is reported to have various hepatoprotective properties. Therefore, a total of 30 natural bioactive compounds obtained from extracts of *Ricinus communis* have been selected for this study, from available literature[11-16].

Target protein structure preparation

The 3D structure of human STAT3 protein (PDB ID: 6TLC) was downloaded from the PDB (protein data bank) website[19]. The BIOVIA Discovery Studio Visualizer was used to remove the water molecules, hetero-atoms, and other related solvent molecules from the structure. Auto Dock Tools (ADT) software version 1.5.7 was utilized to prepare the receptor protein by removing water molecules and bound ligands, then adding hydrogens Kollman atom charges., Gasteiger charges and detecting flexible torsions and setting the number of torsions the r adding polar hydrogens and Non-polar hydrogens were merged[20]. The docking input file, namely the PDBQT file, was generated using the Auto Dock Tool (ADT). The chosen protein underwent no protein relaxation; instead, it was docked as a rigid model structure.

Ligand structure preparation

The ligands used for this docking study were chosen from the literature**.** 30 plant bioactive compounds that are mainly present in the leaves of the plant *Ricinus communis* were considered for the study[17,21,22]. The ligand structure was downloaded from the PUBCHEM database for 3-dimensional optimization. Using the Open Babel program, version 3.1.1, the obtained SDF ligand files which contained all hydrogens were translated to PDB file format. The 3D structure of the ligands that were not available in the PUBCHEM server was created by Marvin-Chemaxon (https://chemaxon.com/marvin) by using their canonical smile. The gasteiger charges were added, non-polar hydrogens were combined, and aromatic carbons were prepared for docking with Auto Dock Tools (ADT). Torsional flexibility of the ligands was granted to enable a wide range of conformational and orientation options.

Active site and grid generation

A grid box encompassing the whole STAT3 protein was created for blind docking. For the X, Y, and Z axes, the grid box sizes were set to 108, 64, and 108, respectively. For X, Y, and Z, the center grid box was defined at 3.605, 27.719, and 34.971, in that order.

Molecular docking

The Auto Dock Vina tool was utilized to predict energetically favorable binding poses between the selected ligands and the STAT3 protein. The docking procedure was performed on a set of 30 phyto-chemicals that were of particular interest. The docking was executed using the local search global optimizer and implemented *via* the broadening Fletcher Goldfarb-Shanno (BFGS) method for local optimization. This also acted as a positive control for the docking simulations. Using a docking exhaustiveness of 8, the software produced nine possesses of the protein-ligand complex, which were subsequently arranged based on their binding affinity[23-25].

Analysis and visualization of docking simulation results

The conformation with the lowest binding affinity was selected for further examination after the docking postures were ranked according to their binding affinities. The BIOVIA Discovery Studio visualizer was used to display the binding poses orientation and conformation as well as the interacting residues, bond kinds, and bond lengths.

Drug likeness and ADME analysis

The pharmacokinetic profile of the drugs of interest with top percentile binding affinity and a binding posture were predicted using the Swiss ADME predictor. The screening of the ligands was additionally conducted, taking into account their physicochemical properties such as lipophilicity and water solubility, pharmacokinetics according to their compliance with Lipinski, Veber, Egan and Mueggerules and medicinal chemistry based on their compliance with lead likeness.

Molecular dynamics (MD) simulation

Molecular dynamics simulation was run for the selected ligand-receptor complex following molecular docking calculations to determine the stability of the protein-ligand complex. The GROMOS 54a7 software was utilized for the molecular dynamic simulation and analysis of the chosen protein-ligand combination. The system was subjected to energy reduction for fifty thousand steps. A protein-ligand complex with solvent simulation system was developed with the use of the GPU-enabled GROMACS 2022 package. The system was extended using the GROMOS 54a7 force field, and the solvent was modeled using a Cubic box and the SPCE water system. To neutralize the systems, 1.5 mM of NaCl ions are added to the water-filled box. Next, the system was used for simulation time set up for 100 ns under normal NTP constant number of particles (N), pressure (P), and temperature (T) conditions where the model system was relaxed before the simulation. The simulation interactive diagram tool further analyzed the simulation data in a graphical way, which provided information of protein-ligand complex properties during the simulation time of 100 ns. Root Mean Square Distance (RMSD), Root Mean Square Fluctuation (RMSF), and H-bond interaction data were analyzed to further validate the findings in docking After that, Radius of gyration (RG), solvent accessible surface area (SASA), root mean square deviation (RMSD), root mean square fluctuation (RMSF) and Binding free energy were calculated for all the generated conformers[26-28].

Binding free energy

The Molecular Mechanic/Poisson-Boltzmann Surface Area (MM-PBSA) method was utilized to calculate the binding energy based on the trajectory of molecular dynamics simulations. This method could more accurately reflect the binding effect of ligand STAT3 target proteins[29]. An effective and trustworthy technique for modeling molecular recognition, such as interactions involving protein-ligand binding, is the MM-PBSA. Using the MMPBSA.py script, the binding free energy was calculated in order to determine the strength of STAT3's binding in complex with either of the potential hits or the reference compound. The following equation was used to calculate the free energy.

G bind = _G complex – [_G receptor + _G ligand]

G bind is defined by the equations as total binding free energies; complex free energies are represented by the ΔG complex; the remaining terms represent the corresponding free energies of the receptor protein and ligand[6].

Results and Discussion

Liver fibrosis is a serious global health problem which can lead to liver cirrhosis or heaptocellular carcinoma[30]. The extracellular matrix (ECM) gradually builds up and damages the liver's physiological architecture, resulting in liver fibrosis[31]. In today’s lifestyle, it is one of the major health issues worldwide. However, there has been no clinically proven effective drug for liver fibrosis till date[32]. Therefore, it is extremely important to explore more effective targets and drugs to control liver fibrosis and to minimize the damage of liver fibrosis.

Molecular docking

The obtained results of molecular docking of potential ligand inhibitors in the 3-dimensional structure of the target protein (STAT3) are presented in (Table 1).

The molecular interactions of the target protein and the bioactive compounds were analyzed by using Auto Dock Vina. Each compound was docked with the target protein and after comparing the docking results, it was found that (5beta)Pregnane-3,20beta-diol, 14alpha,18alpha-[4-methyl-3-oxo-(1-oxa-4-azabutane-1,4-diyl)]-, diacetate (https://pubchem.ncbi.nlm.nih.gov/compound/537242) has the highest scoring function compared to other compounds. Its affinity of binding with the target protein was found to be highest i.e. -8.6 kcal/mol among all the other 30 ligands docked. The interaction between the complex of the STAT3and (5beta)Pregnane-3,20beta-diol, 14alpha,18alpha-[4-methyl-3-oxo-(1-oxa-4-azabutane-1,4-diyl)]-, diacetate was analyzed using Chimera 1.17.1 and BIOVIA Discovery studio visualizer software (Fig. 1).

The results, presented in Table 1, revealed that certain compounds demonstrated significant binding affinities for inhibiting the target protein. Several natural compounds were found which inhibits STAT3 thereby reducing fibrotic markers in liver tissue in preclinical models of liver fibrosis in mice[33,34].

The present study was undertaken to evaluate potential drug candidate against liver fibrosis using bioactive compounds of the plant *Ricinus communis*. Previous studies showed that STAT3 is a therapeutic target for liver fibrosis. The optimal orientation and stability of the protein ligand complex were predicted using molecular docking.(5beta)Pregnane-3,20 beta-diol, 14alpha,18alpha-[4-methyl-3-oxo-(1-oxa-4-

Table 1 — The docking scores of 30 ligands and their interactions with STAT3 protein

Sl. No	Compound Name	Binding Affinity (kcal/mol)	Molecular Weight (g/mol)
1	(5beta)Pregnane-3,20beta-diol, 14alpha,18alpha-[4-methyl-3-oxo-(1-oxa-4-azabutane-1,4-diyl)]-, diacetate	-8.6	489.7
2	Rutin	-8.5	610.51
3	Isoquercetrin	-8.1	464.09
4	Gibberellic Acid	-8	346.4
5	Quercetrin	-7.8	448.4
6	Quercetin	-7.8	302.23
7	Phenol,4-(1,1,3,3-Tetramethylbutyl)-	-6	206.32
8	Triethyl Citrate	-5.8	276.28
9	Diethyl Phthalate	-5.7	222.24
10	Limonene, (+)-	-5.5	136.23
11	Ricinine	-5.4	164.16
12	N DemethylRicinine	-5.2	150.13
13	Geranyl Isovalerate	-5.1	238.37
14	Dodecanoic Acid, 3-Hydroxy-	-4.9	216.32
15	Ribitol	-4.9	152.15
16	Butanedioic Aciod Hydroxyl. Diethyl Esteroror Diethyl Malate	-4.8	190.19
17	DL-Arabinose	-4.6	150.13
18	3-Hydroxydodecanoic Acid	-4.5	216.32
19	3-(N,N-Dimethllaurylammonio) Propanesulfonate	-4.5	335.55
20	P-Dioxane-2,3-Diol	-4.5	120.1
21	Methyl 6-Oxoheptanoate	-4.5	158.19
22	L-Valine, Ethyl Ester	-4.5	145.2
23	Dithiocarbamate-Methyl Isobutyl Ketone Or 23-(N,N-Dimethllaurylammonio) Propanesulfonate	-4.4	191.3
24	Octadecanoic Acid	-4.4	284.5
25	Cetene	-4.3	224.42
26	3 - Octadecene	-4.3	252.5
27	N-Haxadecanoic Acid	-4.2	256.42
28	1,2,3,4-Butanetetrol	-4.2	122.12
29	1-Hexadecene	-4.1	224.42
30	3-Ethoxy-1,2-Propanediol	-3.9	120.15

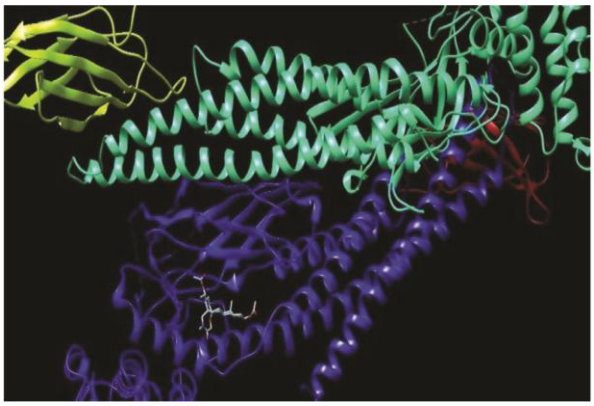

Fig. 1 — Molecular docking analysis of the complex STAT3 and (5beta)Pregnane-3,20beta-diol, 14alpha, 18alpha-[4-methyl-3-oxo-(1-oxa-4-azabutane-1,4-diyl)]-, diacetate

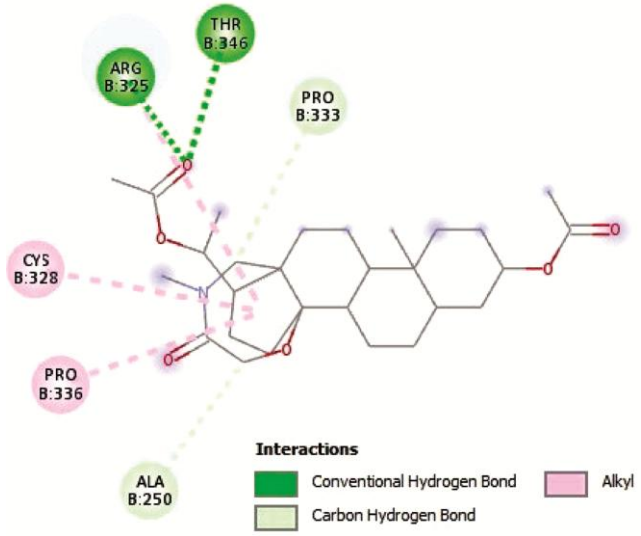

Fig. 2 — The image is a 2D depiction of molecular docking interaction between STAT3 and (5beta)Pregnane-3,20beta-diol, 14alpha,18alpha-[4-methyl-3-oxo-(1-oxa-4-azabutane-1,4-diyl)]-, diacetate

azabutane-1,4-diyl)]-, diacetate exhibited best binding affinity of -8.6 showed Alkyl, conventional hydrogen bond and carbon hydrogen bond with the STAT3 protein. It interacted at THR B:346, ARG B:325,CYS B:328,PRO B:336,ALA B:250, and PRO B:333 amino acid residues of the target protein (Fig. 2).

Swiss ADME analysis

After molecular docking, the 10 compounds with the best docking scores were selected for ADME analysis. The results of the Swiss ADME analysis are provided in (Table 2).

The pharmacokinetic parameters of biologically active compounds are determined by using Swiss ADME. The pharmacokinetics, bioavailability, and toxicity profile of a substance are all significantly influenced by ADME factors. Out of 30 ligands, 10 ligands that had the best docking score were chosen to have their ADME characteristics examined. Among the 10 compounds, ((5beta)Pregnane-3,20beta-diol, 14alpha,18alpha-[4-methyl-3-oxo-(1-oxa-4-azabutane-1,4-diyl)]-, diacetate, was found to be within the limits of the Lipinski, Veber, Egan and Muegge rules satisfying the drug likeness parameter. The compound also fulfilled the Physicochemical parameter, Lipophilicity, Water Solubility, Pharmacokinetics, Medicinal chemistry, rules and parameters. However, other compounds like Rutin, Isoquercetrin, Quercetrin

Table 2 — Swiss ADME screening of selected bioactive compound for drug likeness

	ADME Parameter	
Sl. No	Physicochemical parameter	
1	Formula	C28H43NO6
2	Molecular weight	4.89.64
3	Number of heavy atoms	35
4	Fraction Csp3	0.89
5	Number of aromatic heavy atoms	0
6	Number of rotatable bonds	5
7	Number of H-bond acceptors	16
8	Number of H-bond donors	0
9	Molar refractivity	136.32
10	TPSA	82.14
	Lipophilicity	
11	Log Po/w(iLOGP)	3.9
12	Log Po/w(XLOGP3)	4.02
13	Log Po/w(WLOGP)	3.74
14	Log Po/w(MLOGP)	3.26
15	Log Po/w(SILICOS-IT)	3.69
16	Consensus log P o/w	-5.08
	Water Solubility	
17	Log S(ESOL) Solubility class	-5.08
18	Log S(ALI) solubility class	-5.45
19	Log S(SILICOS-IT)	-4.4
	Pharmacokinetics	
20	GI absorption	High
21	BBB permeant	No
22	P-Gp permeant	No
23	CYP1A2 inhibitor	No
24	CYP2C19 inhibitor	No
25	CYP2C9inhibitor	No
26	CYP3A4inhibitor	No
27	Log Kp (skin permeation)	-6.43
	Drug likeness	
29	Lipinski	0, violation
31	Veber	0, violation
32	Egan	0, violation
33	Muegge	0, violation
34	Bioavailability score	0.55
	Medicinal chemistry	
35	Pains	0 alert
36	Brenk	1 alert
37	Lead likeness	2, violations
38	Synthetic accessibility	6.27

etc. although having good docking score was unable to comply with the above mentioned rules and parameters of ADME. While certain compounds showed violations in different parameters of lead-likeness, no violations were shown by (5beta) Pregnane-3,20beta-diol, 14alpha,18alpha-[4-methyl -3-oxo-(1-oxa-4-azabutane-1,4-diyl)]-, diacetate. It showed signs of high intestine absorption, good bioavailability score, and non-permeability of the blood-brain barrier shown in (Table 2). Based on the docking score and ADME analysis, (5beta)Pregnane-3,20beta-diol, 14alpha,18alpha-[4-methyl-3-oxo-(1-oxa-4-azabutane-1,4-diyl)]-, diacetate, with a bioavailability score of 0.55, was selected for further molecular dynamic simulation which emerged as a strong candidate for developing a new potential drug for liver fibrosis treatment. However, it is necessary to conduct additional research to assess the toxicology, pharmacology, and experimental bioavailability of the compound in order to validate the current predictions.

Molecular dynamic (MD) simulation

Molecular dynamics simulation was performed using the target protein (STAT3) complexed with (5beta)Pregnane-3,20beta-diol, 14alpha,18alpha-[4-methyl-3-oxo-(1-oxa-4-azabutane-1,4-diyl)]-, diacetate, that had the best docking score, superior interactions, binding energies, favorable docking scores, and satisfied ADMET properties were assessed using the following metrics: radius of gyration (RG), solvent accessible surface area (SASA), root mean square deviation (RMSD), root mean square fluctuation (RMSF), H-bond interaction, and binding free energy (MMPBSA). It is employed to comprehend the stability and molecular interaction of the ligand-protein complex.

The RMSD values were determined based on a simulation timescale of 100 ns. The (5beta)Pregnane-3,20beta-diol, 14alpha,18alpha-[4-methyl-3-oxo-(1-oxa-4-azabutane-1,4-diyl)]-, diacetate-STAT3 complex exhibited very stable behavior until 60 ns. From the result, it was found that the complex showed stability throughout the simulation, indicating its comparative stability shown in (Fig. 3). RMSD is used to determine the stability of ligand protein complex. The root mean square deviation of backbone atoms and the amount of backbone hydrogens were used to examine and track the equilibration of MD trajectories produced from the protein-ligand simulation system, as shown in (Fig. 3). In the RMSD analysis, it was observed that the complex of (5β)-Pregnane-3,20β-diol, 14α,18α-[4-methyl-3-oxo-(1-oxa-4-azabutane-1,4-diyl)]-, diacetate with STAT3 remained stable for the first 60 ns. However, after this period, the complex exhibited multiple fluctuations throughout the remainder of the 100 ns trajectory. Notably, between 60 and 70 ns, the RMSD value showed its highest fluctuation, reaching approximately 0.8 nm (as shown in Fig. 3) which indicates that the complex maintained its conformation without significant deviation in the first 60s, but after that the fluctuations indicate that the complex underwent conformational changes, implying a potential loss of stability or alterations in the interaction between the molecules.

The RMSF values were computed within the simulation timescale of 0 to 100 ns. The RMSF values showed a minor fluctuation for the (5beta)Pregnane-3,20beta-diol, 14alpha,18alpha-[4-methyl-3-oxo-(1-oxa-4-azabutane-1,4-diyl)]-, diacetate during the simulation and over all appeared as stable shown in (Fig. 4). RMSF serves as an indicator of protein flexibility, which is useful for characterizing local changes along the protein chain. The portions of the

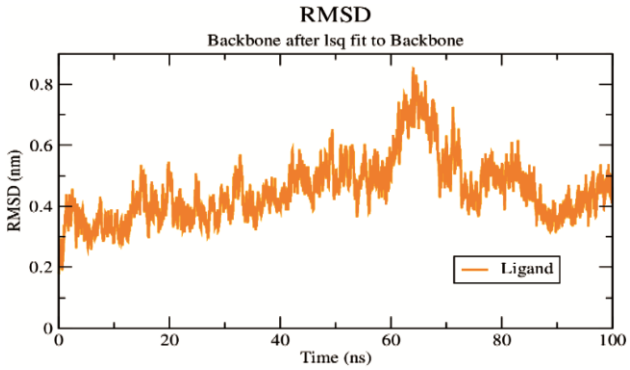

Fig. 3 — Change in the RMSD of the (5beta)Pregnane-3,20beta-diol, 14alpha,18alpha-[4-methyl-3-oxo-(1-oxa-4-azabutane-1,4-diyl)]-, diacetate –STAT3 complex over time during molecular dynamics simulation

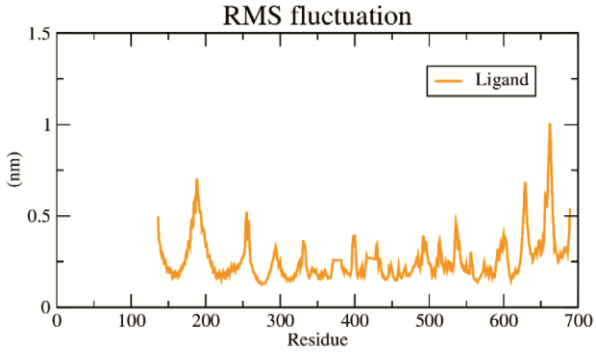

Fig. 4 — RMSF calculated based on molecular dynamics simulation trajectory

protein that fluctuate the most during the simulation are indicated by peaks on this map. The N- and C-terminal tails of the protein have generally been shown to vary more than any other portion of the protein. Compared to the unstructured portion of the protein, secondary structural components such as alpha helices and beta strands are typically more rigid and vary less than loop sections. Usually, after the ligand-protein interaction, the ligand stabilizes the protein and decreases the enzymatic function, forming a stable complex[35].The RMSF of the ligand showed minimal fluctuations in the graph. The highest pick observed in the graph was 1nm. It indicates that binding of (5beta)Pregnane-3,20beta-diol, 14alpha, 18alpha-[4-methyl-3-oxo-(1-oxa-4-azabutane-1,4-diyl)]-, diacetate STAT3 could be a stable, complex (Fig. 4).

The mass-weighted root mean square distance of atoms from their centre of mass is known as the RG. The complex showed a consistent trend of RG value from 0 to 100ns throughout the simulation. The result indicates that the complex was very compact and stable shown in (Fig. 5). Rg plot exposed the compactness and unwinding of STAT3 with respect to the ligand (5beta)Pregnane-3,20beta-diol, 14alpha, 18alpha-[4-methyl-3-oxo-(1-oxa-4-azabutane-1,4-diyl)]-, diacetate. The distribution of atoms along a protein's axis is known as its Rg. The length is a measure of how far something is rotated from the point at which energy transmission is most effective. The compound was found to exhibit an extremely compact structure based on the results. The Rg value of the complex was around 3.4-3.7 nm, which indicates that the complex will be extremely stable and compact (Fig. 5).

The overall free binding energy and the polar solvation energy, however, had a positive interaction. The complex's binding free energy ΔG Bind (5beta).

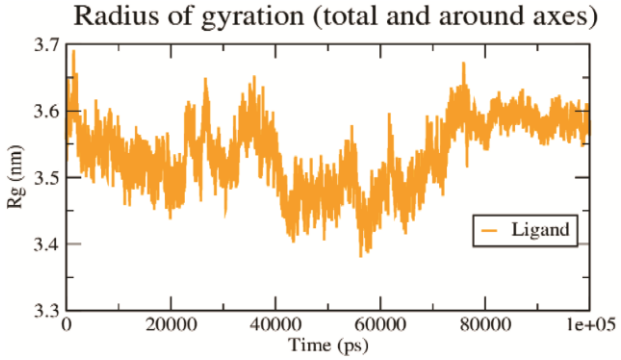

Fig. 5 — RG of back bone atoms of (5beta)Pregnane-3,20beta-diol, 14alpha,18alpha-[4-methyl-3-oxo-(1-oxa-4-azabutane-1,4-diyl)]-, diacetate

The values of -143.102 +/- 5.282 kJ/ for (5beta) Pregnane-3,20beta-diol, 14alpha,18alpha-[4-methyl -3-oxo-(1-oxa-4-azabutane-1,4-diyl)]-, diacetate-STAT3 were determined by a 100 ns simulation. The term "surface area accessible to surrounding molecules" (SASA) describes a bio molecule's ability to provide information about its structural and functional characteristics. It can also suggest regions where the ligand binds to the protein. From (Fig. 6), it was observed that most of the interactions were in the area between 280 and 295 nm, which suggests the highest interaction between the target and the ligand in this region.

The H-bond timeline in Figure 7 is a representation of the interactions and contacts (H-bonds). A deeper shade of black indicates that some residues establish many specific contacts with the ligand during the MD trajectories. The overall free binding energy and the polar solvation energy, however, had a positive interaction. The values of -143.102 +/- 5.282 kJ/ for (5beta)Pregnane-3,20beta-diol, 14alpha,18alpha-[4-methyl-3-oxo-(1-oxa-4-azabutane-1,4-diyl)]-, diacetate-

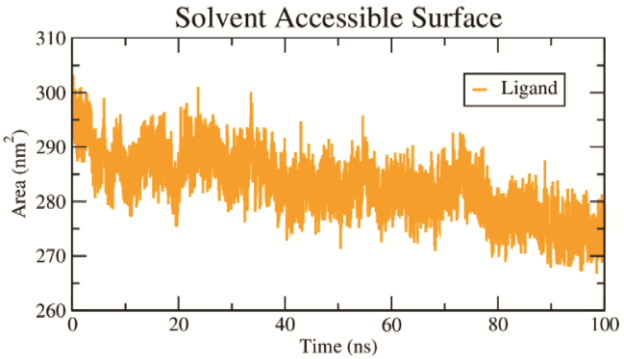

Fig. 6 — SASA of back bone atoms of (5beta)Pregnane-3,20beta-diol, 14alpha,18alpha-[4-methyl-3-oxo-(1-oxa-4-azabutane-1,4-diyl)]-, diacetate–STAT3

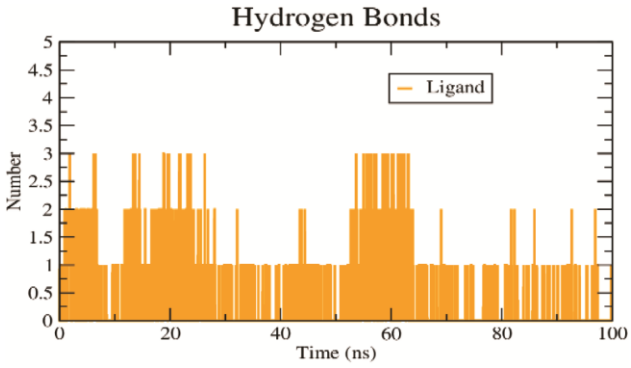

Fig. 7 — Variations in the quantity of hydrogen bonds formed between proteins and small molecules throughout the molecular dynamics simulation process

STAT3 were determined by a 100 ns simulation. From Figure 7, it was observed that the complex forms a large number of H bonds, which depicts a stable complex and strong interaction between the ligand and the protein.

Binding free energy

Using the MMPBSA technique, the binding energy of the target protein STAT3 was determined. For the STAT3 protein van der Waal energy and Electrostatic energy contributed negatively to the total interaction which is founded to be -201.834 +/- 10.716 kJ/mol and -11.870+/-3.188 kJ/mol, respectively. Nonetheless, there was a positive interaction between the total free binding energy and the Polar solvation energy. The complex(5.beta) binding free energies ΔG During the 100 ns simulation, the values of -143.102 +/- 5.282 kJ/ for (5beta)Pregnane-3,20beta-diol, 14alpha, 18alpha-[4-methyl-3-oxo-(1-oxa-4-azabutane-1,4-diyl)]-, diacetate-STAT3 were determined.

Binding free energy (Kcal/mol) was calculated for the (5beta)Pregnane-3,20beta-diol, 14alpha,18alpha-[4-methyl-3-oxo-(1-oxa-4-azabutane-1,4-diyl)]-, diacetate and STAT3 complex using MMPBSA based on 100 ns MD trajectory. The overall free binding energy was positively impacted by the polar solvation energy and adversely by the van der Wall and electrostatic energies. The binding energy of (5beta)Pregnane-3,20beta-diol, 14alpha,18alpha-[4-methyl-3-oxo-(1-oxa-4-azabutane-1,4-diyl)]-, diacetate to STAT3 was found to be -143.102 +/- 5.282 kJ/mol, which is an indication of strong binding energy. A robust binding energy indicates that the ligand and protein are interacting steadily. It implies that the protein and ligand are firmly bonded, making it less likely for the ligand to break out from its binding site.

Conclusion

The potential of bioactive compounds from *Ricinus communis* against the STAT3 protein has proved valuable insights into their pharmacological properties. Additionally, a total of 30 active compounds were selected from *Ricinus communis* from available literature. However, through computational analysis, it was observed that the best promising compound was (5beta)Pregnane-3,20 beta-diol, 14alpha,18alpha-[4-methyl-3-oxo-(1-oxa-4-azabutane-1,4-diyl)]-, diacetate with favorable binding affinities, drug-likeness and pharmacokinetic profile, suggesting their potential as a lead candidate. To confirm the effectiveness and safety of these drugs, more *in vitro* and in vivo research is required. This might pave the way for the creation of new therapies to treat STAT3-associated diseases.

Acknowledgement

The authors kindly acknowledge the financial support as studentship to Ms. Doli Saloi from the Department of Biotechnology (DBT), Government of India.

Conflicts of Interest

All authors declare no conflicts of interest.

References

1 Friedman SL, Liver fibrosis from bench to bedside. *J Hepatol*, 38 (2003) 38.
2 Bataller R & Brenner DA, Liver fibrosis. *J Clin Invest*, 115.2 (2005) 209.
3 Higashi T, Friedman SL & Hoshida Y, Hepatic stellate cells as key target in liver fibrosis. *Adv Drug Deliv Rev*, 121 (2017) 27.
4 Wells RG, The portal fibroblast: not just a poor man's stellate cell. *Gastroenterology*, 147.1 (2014) 41.
5 Wang Z, Long J & Zhang H, The STAT3 inhibitor S3I-201 suppresses fibrogenesis and angiogenesis in liver fibrosis. *Lab Invest*, 98.12 (2018) 1600.
6 Rafiq H, Hu J, Hakami MA, Hazazi A, Alamri MA, Alkhatabi HA, Mahmood A, Alotaibi BS, Wadood A & Huang X, Identification of novel STAT3 inhibitors for liver fibrosis, using pharmacophore-based virtual screening, molecular docking, and biomolecular dynamics simulations. *Sci Rep*, 13 (2023) 20147.
7 Zhang XQ, Jiang L, You JP, Liu YY, Peng J, Zhang HY, Xu BY & Mao Q, Efficacy of short-term dexamethasone therapy in acute-on-chronic pre-liver failure. *Hepatol Res*, 41 (2011) 46.
8 Xu S, Wang Y, Tai DC, Wang S, Cheng CL, Peng Q, Yan J, Chen Y, Sun J, Liang X & Zhu Y, q Fibrosis: a fully-quantitative innovative method incorporating histological features to facilitate accurate fibrosis scoring in animal model and chronic hepatitis B patients. *J Hepatol*, 61 (2014) 260.
9 Ojezele MO, Comparative evaluation of the effects of n-hexane, chloroform, and methanol fractions of *Ricinus communis* in carbon tetrachloride-induced hepatotoxic rats. *Thai J Pharm Sci*, 44 (2020) 1.
10 Shukla B, Visen PK, Patnaik GK, Kapoor NK & Dhawan BN, Hepatoprotective effect of an active constituent isolated from the leaves of *Ricinus communis* Linn. *Drug Dev Res*, 26 (1992) 183.
11 Babu PR, Bhuvaneswar C, Sandeep G, Ramaiah CV & Rajendra W, Hepatoprotective role of *Ricinus communis* leaf extract against d-galactosamine induced acute hepatitis in albino rats. *Biomed Pharmacother*, 88 (2017) 658.
12 Ayyanar M & Ignacimuthu S, Traditional knowledge of kanitribals in Kouthalai of Tirunelveli hills, Tamil Nadu, India. *J Ethnopharmacol*, 102 (2005) 246.

13 Baruah M & Kalita D, Ethnomedicine used by Mishings tribes of Dibrugarh district, Assam. *Indian J Tradit Know*, 64 (2007) 595.
14 Visen PK, Shukla B, Patnaik GK, Tripathi SC, Kulshreshtha DK, Srimal RC & Dhawan BN, Hepatoprotective activity of *Ricinus communis* leaves. *Int J Pharmacogn*, 30 (1992) 241.
15 McMillan JM & McMillan DC, S-adenosylmethionine but not glutathione protects against galactosamine-induced cytotoxicity in rat hepatocyte cultures. *Toxicology*, 222 (2006) 175.
16 Jena J & Gupta AK, *Ricinus communis* Linn: a phyto-pharmacological review. *Int J Pharm Pharm Sci*, 4 (2012) 25.
17 Kumar M, A review on phytochemical constituents and pharmacological activities of *Ricinus communis* L. *Plant Int J Pharmacogn Phytochem Res*, 9 (2017) 466.
18 Agarwal S & Mehrotra RJ, An overview of molecular docking. *JSM Chem*, 4 (2016) 1024.
19 Hussain S, Mustafa G, Ahmed S & Albeshr MF, Underlying mechanisms of *Bergenia* spp. to treat hepatocellular carcinoma using an integrated network pharmacology and molecular docking approach. *Pharmaceuticals*, 16 (2023) 1239.
20 Cakmak S & Erdogan T, Some bis (3-(4-nitrophenyl) acrylamide derivatives: Synthesis, characterization, DFT, antioxidant, antimicrobial properties, molecular docking and molecular dynamics simulation studies. *Indian J Biochem Biophys*, 60 (2023) 209.
21 Hussein AO, Hameed IH, Jasim H & Kareem MA. Determination of alkaloid compounds of *Ricinus communis* by using gas chromatography-mass spectroscopy (GC-MS). *J Med Plants Res*, 9 (2015) 349.
22 Hussein HM, Hameed RH & Hameed IH, Screening of bioactive compounds of *Ricinus communis* using GC-MS and FTIR and evaluation of its antibacterial and antifungal activity. *Indian J Public Health Res Dev*, 9 (2018) 463.
23 Jyothi K, Sivaranjani V, Pavithra U, Jayavel S & Muthulakshmi L, Computational studies on new Leishmanial drug targets against Quercetin. *Indian J Biochem Biophys*, 59 (2022): 909.
24 Ganeshpurkar A, Chaturvedi A, Shrivastava A, Dubey N, Jain S, Saxena N, Gupta P & Mujariya R, *In silico* interaction of Berberine with some immunomodulatory targets: A docking analysis. *Indian J Biochem Biophys*, 59 (2022) 848.
25 Matilda JJ & Reji TA, Design, structural characterization, biological evaluation and molecular docking studies of methylindole bearing thiocarbamoylpyrazole moieties. *Indian J Biochem Biophys*, 61 (2024) 418.
26 Nalban N, Matte S, Jamadagni P & Tamboli M, A comprehensive computational study of Millets derived phytochemicals as potential inhibitors of NACHT domain of NLRP3 inflammasome: Molecular docking, molecular dynamics simulation, MM-PBSA free energy calculation and DFT analysis. *Indian J Biochem Biophys*, 61 (2024) 223.
27 Santh Rani T, PremithaRajya Lakshmi P & Manga Devi C, Network pharmacology and molecular docking study of the active ingredients in Saptasaramkashayam for the treatment of Polycystic ovary syndrome. *Indian J Biochem Biophys*, 60 (2023) 108.
28 Goel S & Kumar Y, Assessing inhibitory potential of natural compounds against BACE1 in Alzheimer's disease: A molecular docking and molecular dynamics simulation approach. *Indian J Biochem Biophys*, 61 (2024) 345.
29 Aydın MM & Akçalı KC. Liver fibrosis. *Turk J Gastroenterol*, 29 (2018) 14.
30 Roehlen N, Crouchet E & Baumert TF, Liver fibrosis: Mechanistic concepts and therapeutic perspectives. *Cells*, 9 (2020) 875.
31 Wang SJ, Ye W, Li WY, Tian W, Zhang M, Sun Y, Feng YD, Liu CX, Liu SY, Cao W & Meng JR, Effects and mechanisms of Xiaochaihu Tang against liver fibrosis: An integration of network pharmacology, molecular docking and experimental validation. *J Ethnopharmacol*, 303 (2023) 116053.
32 Zhao J, Qi YF & Yu YR, STAT3: A key regulator in liver fibrosis. *Ann Hepatol*, 21 (2021) 100224.
33 Wen W, Wu J, Liu L, Tian Y, Buettner R, Hsieh MY, Horne D, Dellinger TH, Han ES, Jove R & Yim JH, Synergistic anti-tumor effect of combined inhibition of EGFR and JAK/STAT3 pathways in human ovarian cancer. *Mol Cancer*, 14 (2015) 1.
34 Song TL, Nairismägi ML, Laurensia Y, Lim JQ, Tan J, Li ZM, Pang WL, Kizhakeyil A, Wijaya GC, Huang DC & Nagarajan S, Oncogenic activation of the STAT3 pathway drives PD-L1 expression in natural killer/T-cell lymphoma. *Blood*, 132 (2018) 1146.
35 Jiang T, Chen X, Yang W, Li N, Xu J, Lu Y, Zhang S, Yu S & Li Y, Network pharmacology, molecular docking, molecular dynamics simulation, and *in vitro* experiments to explore the mechanism of Asiatic acid inhibiting acetaldehyde-induced activation of hepatic stellate cells. *Nat Prod Commun*, 18 (2023) 1.